Effective Multistep Exciton Delivery Through DNA-based Photonic Wires

C.M. Spillmann,[*,a] S. Buckhout-White,[*,b] M.G. Ancona,[**,c] P.D. Cunningham,[**,d] J.S. Melinger,[**,e] E.R. Goldman,[*,f] I.L. Medintz[*,g]

[*]Center for Bio/Molecular Science and Engineering, [**]Electronics Science and Technology Division, Naval Research Laboratory, 4555 Overlook Ave SW, Washington, DC 20375;
[a]christopher.spillmann@nrl.navy.mil; [b]susan.buckhout-white@nrl.navy.mil; [c]mario.ancona@nrl.navy.mil; [d]paul.cunningham@nrl.navy.mil; [e]joseph.melinger@nrl.navy.mil; [f]ellen.goldman@nrl.navy.mil; [g]igor.medintz@nrl.navy.mil;

ABSTRACT

DNA demonstrates a capacity for creating designer nanostructures. A number of these utilize Förster resonance energy transfer (FRET) as part of the devices functionality. As device sophistication increases so do the FRET requirements. Here we report on multi-dye FRET cascades consisting of DNA with pendant organic dyes as nanoantennae that focus excitonic energy. We evaluate 36 DNA designs including linear, bifurcated, Holliday junction, 8-arm star, and dendrimers involving up to five-dyes engaging in four-consecutive FRET steps while systematically varying fluorophore spacing by Förster distance (R_0). Decreasing R_0 while augmenting with multiple donors significantly increases terminal exciton delivery efficiency within dendrimers compared to the linear constructs. Förster modeling confirms that best results are obtained when there are multiple parallel FRET pathways rather than independent channels by which excitons travel from initial donor(s) to final acceptor.

Keywords: photonic wire, DNA, energy transfer, exciton, fluorophore

1 INTRODUCTION

Structural DNA technology is now used to create nano-assemblies with multi-dimensional shapes. As a result, several DNA-based applications are being developed. This is possible because of the canonical Watson-Crick base pairing and the fact that DNA can be custom-synthesized and site-specifically modified with chemical moieties such as organic fluorophores [1, 2]. A number of these structures incorporate multiple dyes and rely on FRET as part of the optical function or to interrogate the assembly itself. FRET is dependent on several factors including the inter-fluorophore spacing, the spectral overlap of the donor emission with the acceptor absorption, and quantum yield of the donor (see Eqs. 1-3). Applications where DNA-based FRET have been demonstrated or exhibit strong potential include molecular computing, biosensing, and light harvesting [3-8]. As DNA devices grow more sophisticated so also will the FRET requirements. Thus it is important to understand how complex FRET networks assemble on DNA scaffolds and what functional constraints are imposed.

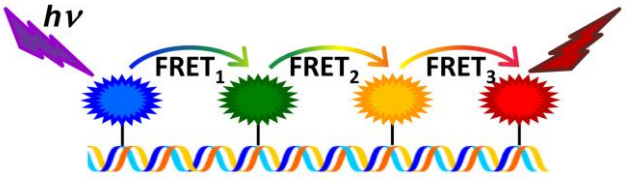

Fig. 1: General scheme of FRET through a multi-fluorophore DNA photonic wire.

The most advanced use of DNA-organized fluorophores and FRET has been photonic wires in which dyes are arranged for directed or sequential energy transfer (Fig. 1). A typical design involves 3-6 dyes attached to DNA at separations typically less than their Förster distances, R_0, [9] defined below and related to the transfer efficiency, E, as:

$$R_0^6 = \frac{K_F \kappa^2 \Phi_D J}{n^4 N_A} \quad (1)$$

$$E = \frac{R_0^6}{R_0^6 + r_{DA}^6} \quad (2)$$

where K_F is a constant, κ^2 is the dipole orientation factor, Φ_D is the quantum yield of the donor, n is the refractive index of the medium, and N_A is Avagadro's number. The value J is the spectral overlap integral defined as:

$$J = \int f_D(\lambda)\,\varepsilon_A(\lambda)\lambda^4 d\lambda \quad (3)$$

where f_D is the normalized donor emission spectrum and ε_A is the acceptor molar extinction coefficient integrated as a function of the wavelength, λ. We note that R_0 corresponds to a donor-acceptor distance where E is equal to 50%. The sensitivity of FRET to the donor-acceptor spacing is highlighted by the r^6 dependence and has been used traditionally as a spectroscopic ruler.

Here, we utilize the flexibility of DNA architecture to move beyond linear photonic wires to achieve more

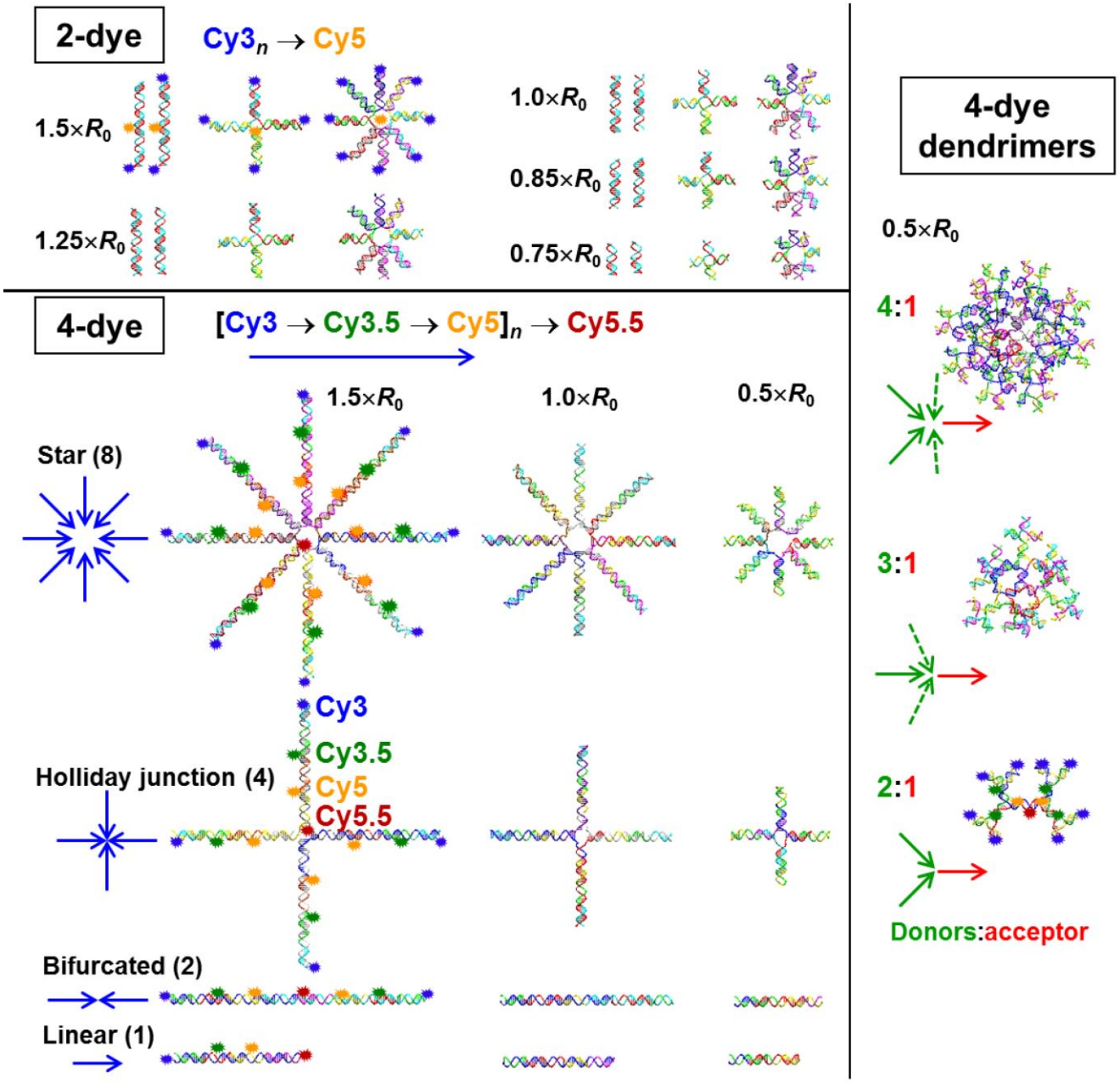

Figure 2. Overview of DNA-fluorophore constructs consisting of 2-dye and 4-dye linear and branched structures with various inter-dye spacings. Adapted from ref. [10].

sophisticated DNA-arranged networks involving as many as 85 organic dye molecules engaged in programmable FRET cascades. We evaluate the performance of 36 antenna designs of increasing complexity (Fig. 2) by assembling >550 different DNA constructs consisting of several control structures of each design. These include linear, bifurcated, Holliday junction, 8-arm star, and 2:1, 3:1, or 4:1 branching dendrimers with either two- or four-dye types, engaged in one-, three-, or four-consecutive FRET steps, respectively, where inter-fluorophore spacings are systematically varied in increments of R_0. The fluorophores used were the cyanine dyes Cy3, Cy3.5, Cy5, and Cy5.5. Details of the materials, structure design, experimental methods, experimental analysis, and Förster modeling are provided elsewhere [10].

2 RESULTS

Fluorescence spectra of the constructs were obtained by illuminating the samples at a wavelength primarily exciting the initial (Cy3) donors and collecting photoluminescent (PL) output. Data of constructs with all dyes present and control structures with different dye positions absent were collected to assess all the FRET pathways. A set of experiments showing the FRET evolution of 3 constructs as an additional terminal dye is added to the system is illustrated in Figure 3 for the linear 4-dye construct with $0.5\times R_0$ inter-dye spacing between each FRET pair (Fig.

3A), the 0.5×R_0 8-armed star (Fig. 3B), and the 0.5×R_0 2:1 dendrimer (Fig. 3C). In each, as the system is built up from the primary donor Cy3 to two dyes (Cy3-Cy3.5), three dyes (Cy3-Cy3.5-Cy5), and the full 4-dye construct (Cy3-Cy3.5-Cy5-Cy5.5), the spectra show sequential quenching of the donor PL peaks and concomitant sensitization of the terminal acceptor, indicating FRET.

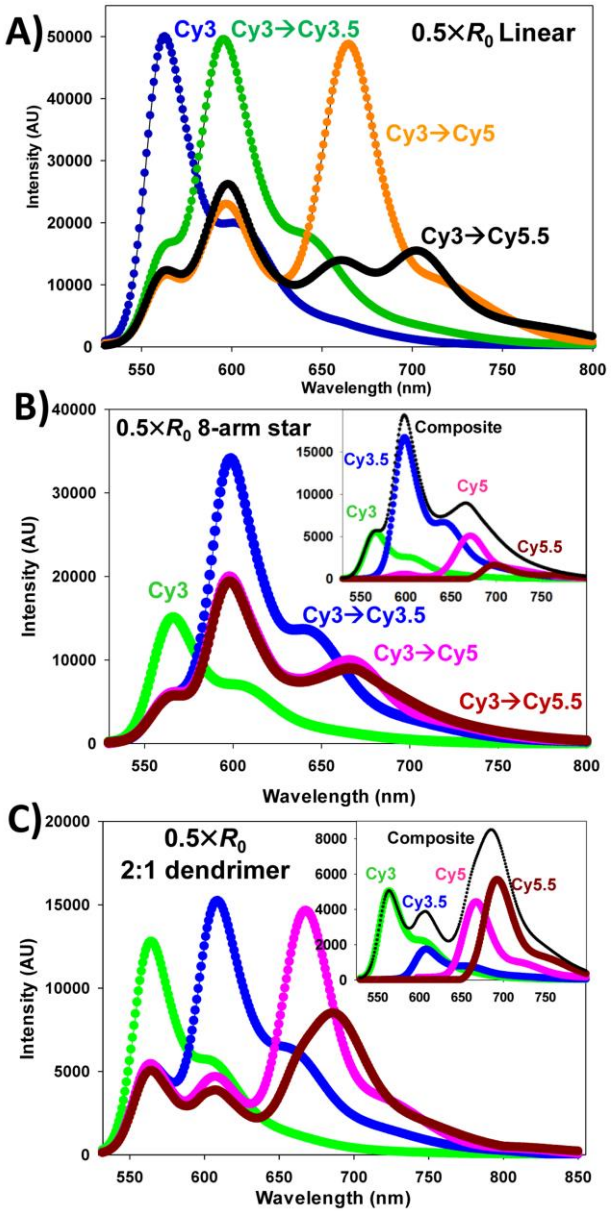

Fig. 3. PL spectra of select constructs. A) FRET evolution of 0.5×R_o linear wire with 1 (blue), 2 (green), 3 (orange), and 4 dyes (black) present. FRET evolution of B) 0.5×R_o 8-arm star and D) 2:1 dendrimer with 1 (green), 2 (blue), 3 (pink), and 4-dyes (dark red) present. Insets: Individual PL contributions from each fluorophore from the complete 4-dye construct. Adapted from ref. [10].

In the full 4-dye linear construct (Fig. 3A, black curve), the PL peak rising at ~700 nm is emission from the terminal Cy5.5 fluorophore, demonstrating a complete cascade of energy along the wire. Figure 3B, C show the same evolution as in Fig. 3A but for a 0.5×R_0 8-arm star and a 2:1 donor-acceptor dendrimer, respectively. As additional fluorophores are added, significant differences are observed in acceptor sensitization. The insets of each plot show the deconstructed contribution from each fluorophore in the full Cy3-Cy3.5-Cy5-Cy5.5 construct and highlight the different PL contributions from each fluorophore. These are important insights into the effectiveness of energy transport since both constructs have the same number of initial Cy3 donors (8) and a single Cy5.5 terminal acceptor. The main difference is that one is composed of 8 independent wires (Fig. 3B) and the other has 2:1 branching of each fluorophore (Fig. 2, 3C). These representative curves demonstrate that critical information is obtained from decomposition of the ensemble PL spectra from various constructs to measure the effect of changes in scaffold design and the inter-fluorophore spacing.

3 ANALYSIS

The data is analyzed in a number of ways to assess performance and gain perspective on optimizing energy throughput across the fluorophores pendent on the DNA scaffolds. One approach is to compare the terminal enhancement factor (TEF). This value is defined as the ratio of the PL intensity of the terminal acceptor (Cy5.5) of each complete 4-dye structure of a particular construct with respect to reference structure; the linear construct with 1.5×R_0 spacing between FRET pairs is the reference.

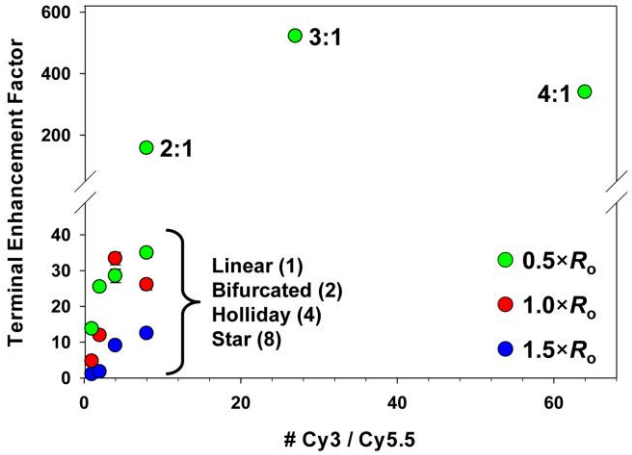

Fig 4. TEF versus the number of initial donors (Cy3) per terminal acceptor (Cy5.5). Reference structure is the 1.5×R_o linear construct. Adapted from ref. [10].

In Fig. 4, TEF is shown versus the number of Cy3 dyes (primary donor) per Cy5.5 dye (terminal acceptor). For all non-dendrimer constructs (linear, bifurcated, Holliday, and 8-arm star), there is an increase in TEF as the number of primary donors is increased and these follow an expected trend when grouped according to the donor-acceptor spacing (Fig. 4, blue, red, green data points in lower left). The constructs with closer-spaced fluorophores are more efficient at energy transfer than those further separated.

When considering the dendrimeric structures, the values of TEF increases dramatically. For example, the 3:1 constructs TEF is over 500× greater than that of the linear 1.5×R_0 construct. Note the comparison of TEF in the 8-way (star) 0.5×R_0 and 2:1 dendrimer constructs. Highlighting the data in Fig. 3B,C, there is large increase in TEF in the latter despite having the same number of primary donors and fewer intermediaries. This is a striking example of how DNA can pattern molecular dyes to significantly alter the fluorescent output. Note the fall off in TEF in the 4:1 dendrimer. Gel electrophoresis and fast protein liquid chromatography revealed low strucutral yield as the primary source of its poor performance.

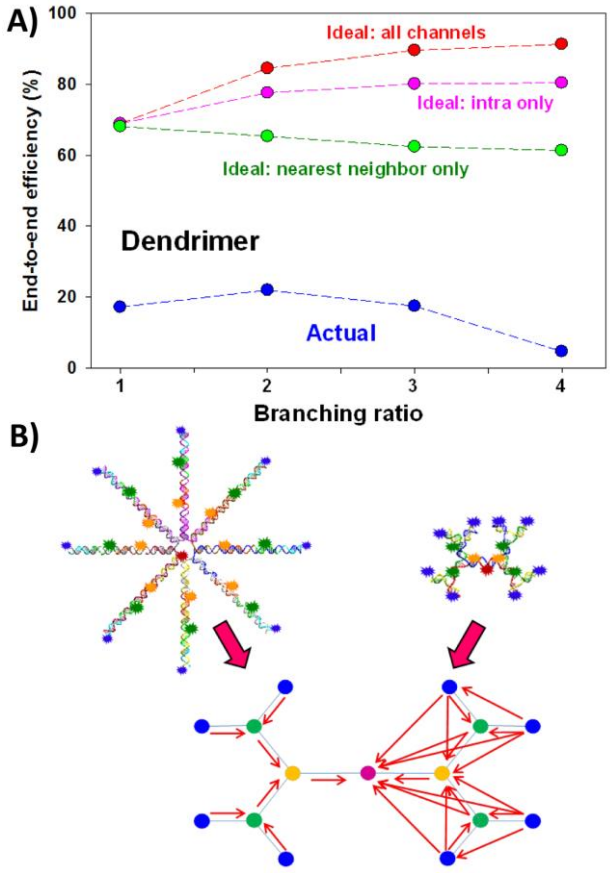

Fig. 5. A) End-to-end efficiency vs. branching ratio of the actual (blue) and model dendrimers with energy transfer between nearest neighbor dyes (green), dyes on the same branch (pink), and all channels (red). B) Schematic of FRET along independent channels (left) vs. multiple interacting pathways (right). Adapted from ref. [10].

Monte Carlo simulations of the constructs based on detailed physical models and Förster theory were carried out to provide insight into the energy transfer processes, sources of non-ideality, and overall system performance. The models accounted for several factors including DNA and dye linker flexibility, incomplete structural yield, homoFRET, etc. One outcome from this analysis is shown in Figure 5, where the end-to-end efficiency, *i.e.* throughput of the system accounting for the quatum yield of the priomary donor and terminal acceptor [10], of dendrimer structures is plotted against the branching ratio. The blue curve is the observed efficiency and green, pink, and red curves are computed based on Förster theory models. The largest source of discrepancy is the yield of fully formed structures. Within the computed data curves, enhanced efficiency is shown when more FRET channels are avaliable. with interactions between dyes on the same branch (Fig. 5A, pink curve; 5B, right) versus a structure acting as several independent channels (Fig. 5A, green curve; 5B, left). An ideal fully formed structure with all possible FRET channels (both intra- and inter-branch) interacting, the efficiency of excitation transfer through the multi-fluorophore structure is predicted to be ~90%. Thus, multiple paths contribute to efficiency enhancement meaning that even improperly formed dendrimer structures, with their overlapping pathways, will be more efficient than several independent photonic wires.

4 CONCLUSION

Optimizing dye placement by decreasing R_0 while increasing effective collection area with multiple initial donors in different geometries provides for >500-fold increase in terminal exciton delivery efficiency within dendrimer structures in direct comparison to the linear 4-dye construct placed at 1.5×R_0. Detailed Förster modeling reveals that crucial to the enhancement is the number of FRET pathways, with best results observed when there are multiple parallel rather than independent channels by which excitons travel from initial donor(s) to final acceptor. These studies also reveal certain non-idealities that appear to be explainable by formation inefficiency, inadequate fluorophore performance and a lack of control over dye orientation. Our results suggest design criteria by which increasingly sophisticated FRET-based DNA devices may be achievable.

5 ACKNOWLEDGEMENTS

The authors acknowledge the Office of Naval Research and the NRL Nanosciences Institute for funding.

REFERENCES

[1] Buckhout-White, S., et al., ACS Nano, 2012, **6**:1026.
[2] Sapsford, K.E., et al., Chem. Rev., 2013, **113**:1904.
[3] Algar, W.R., et al., Anal. Chem., 2012, **84**:10136.
[4] Algar, W.R., et al., JACS, 2012, **134**:1876.
[5] Boeneman, K., et al., JACS, 2010, **132**:18177.
[6] Claussen, J.C., et al., Nanoscale, 2013, **5**:12156.
[7] Claussen, J.C., et al., ACS Appl. Mater. & Interf., 2014, **6**:3771.
[8] Spillmann, C.M., et al., ACS Nano, 2013, **7**:7101.
[9] Medintz, I. and N. Hildebrandt, eds. *FRET - Förster Resonance Energy Transfer*. 2014, Wiley-VCH, Verlag GmbH & Co. KGaA.
[10] Buckhout-White, S., et al., Nat. Commun., 2014, **5**:5615.